

# CUE-RAG: Towards Accurate and Cost-Efficient Graph-Based RAG via Multi-Partite Graph and Query-Driven Iterative Retrieval

Yaodong Su  
yaodongsu@link.cuhk.edu.cn  
The Chinese University of Hong  
Kong, Shenzhen

Yixiang Fang\*  
fangyixiang@cuhk.edu.cn  
The Chinese University of Hong  
Kong, Shenzhen

Yingli Zhou  
yinglizhou@link.cuhk.edu.cn  
The Chinese University of Hong  
Kong, Shenzhen

Quanqing Xu  
xuquanqing.xqq@oceanbase.com  
OceanBase, Ant Group

Chuanhui Yang  
rizhao.ych@oceanbase.com  
OceanBase, Ant Group

## Abstract

Despite the remarkable progress of Large Language Models (LLMs), their performance in question answering (QA) remains limited by the lack of domain-specific and up-to-date knowledge. Retrieval-Augmented Generation (RAG) addresses this limitation by incorporating external information, often from graph-structured data. However, existing graph-based RAG methods suffer from poor graph quality due to incomplete extraction and insufficient utilization of query information during retrieval. To overcome these limitations, we propose CUE-RAG, a novel approach that introduces (1) a multi-partite graph index incorporates text Chunks, knowledge Units, and Entities to capture semantic content at multiple levels of granularity, (2) a hybrid extraction strategy that reduces LLM token usage while still producing accurate and disambiguated knowledge units, and (3) Q-Iter, a query-driven iterative retrieval strategy that enhances relevance through semantic search and constrained graph traversal. Experiments on three QA benchmarks show that CUE-RAG significantly outperforms state-of-the-art baselines, achieving up to 99.33% higher Accuracy and 113.51% higher F1 score while reducing indexing costs by 72.58%. Remarkably, CUE-RAG matches or outperforms baselines even without using an LLM for indexing. These results demonstrate the effectiveness and cost-efficiency of CUE-RAG in advancing graph-based RAG systems.

## Keywords

Graph-based RAG, Multi-Partite Graph, Query-Driven Iterative Retrieval

### ACM Reference Format:

Yaodong Su, Yixiang Fang, Yingli Zhou, Quanqing Xu, and Chuanhui Yang. 2018. CUE-RAG: Towards Accurate and Cost-Efficient Graph-Based RAG via Multi-Partite Graph and Query-Driven Iterative Retrieval. In . ACM, New York, NY, USA, 14 pages. <https://doi.org/XXXXXXXX.XXXXXX>

\*Yixiang Fang is the corresponding author.

Permission to make digital or hard copies of all or part of this work for personal or classroom use is granted without fee provided that copies are not made or distributed for profit or commercial advantage and that copies bear this notice and the full citation on the first page. Copyrights for components of this work owned by others than the author(s) must be honored. Abstracting with credit is permitted. To copy otherwise, or republish, to post on servers or to redistribute to lists, requires prior specific permission and/or a fee. Request permissions from [permissions@acm.org](mailto:permissions@acm.org).  
*Conference'17, Washington, DC, USA*

© 2018 Copyright held by the owner/author(s). Publication rights licensed to ACM.  
ACM ISBN 978-1-4503-XXXX-X/2018/06  
<https://doi.org/XXXXXXXX.XXXXXX>

## 1 Introduction

Large Language Models (LLMs) like Qwen3 [42], DeepSeek [7], and LLaMA3.1 [12] have received tremendous attention from both industry and academia [11, 19, 21, 27, 39]. Despite their remarkable success in question-answering (QA) tasks, they may still generate wrong answers due to a lack of domain-specific and real-time updated knowledge outside their pre-training corpus [30]. To enhance the trustworthiness and interpretability of LLMs, Retrieval-Augmented Generation (RAG) methods [9, 10, 18, 19, 40, 44, 47] have emerged as a core approach, which often retrieve relevant information from documents, relational data, and graph data to facilitate the QA tasks. The state-of-the-art (SOTA) RAG approaches often use the graph data as the external data since they capture the rich semantic information and link relationships between entities.

In the literature, representative graph-based RAG methods typically follow a two-phase pipeline: (1) *Offline graph construction*: The external text corpora  $\mathcal{T}$  are first segmented into smaller chunks, from which nodes and edges are extracted using LLMs to build a knowledge graph (KG) [41, 48]. (2) *Online retrieval*: Given an online query  $q$ , it either retrieves relevant nodes, edges, or subgraphs from the KG for direct answer generation, or optionally traces these elements back to their source text chunks via associated provenance links to support answer generation [8, 13, 14]. While they offer improved performance, both approaches suffer from two major limitations:

**Limitation 1: Poor graph quality.** As shown in recent studies [41, 48], constructed KGs often suffer from incompleteness, typically due to missing key nodes, edges, or the omission of information that cannot be incorporated into structured graph elements. Take the text chunk shown in Figure 1 as an example. Existing methods typically extract only a few triples (e.g.,  $\langle \text{Barcelona, won, Copa del Rey first leg against Getafe} \rangle$ ), while completely ignoring valuable textual information, such as nuanced comparisons between Messi's performance and Maradona's "Goal of the Century". This incompleteness may lead to retrieval errors, to be more specific, when a query involving this detail is issued, the constructed graph fails to provide sufficient information for generating an accurate answer, as shown in Figure 1.

**Limitation 2: Insufficient utilization of the query information.** Most existing methods [8, 13, 14, 20] for online retrieval follow two steps: (1) use the input query to identify relevant elements (e.g., nodes, edges) in the KG, and (2) retrieve additional information based on the above elements, such as text chunks or

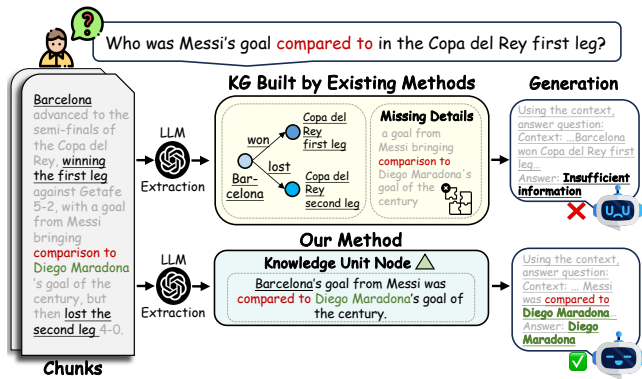


Figure 1: Comparison of our extraction method (Below) and rigid triple extraction in existing Graph-based RAG methods (Upper).

subgraphs, to augment the context for answer generation. While the first step ensures query relevance, the second step often fails to fully leverage the query information, resulting in a semantic misalignment between the query and the retrieved context.

To address **Limitation 1**, we introduce the novel concept of *knowledge unit*, a statement that conveys an atomic piece of information from a text chunk. Collectively, these knowledge units can fully reconstruct the semantic content of the original text. By extracting entities from the knowledge units, we can effectively address missing nodes or edges in the constructed graph. This leads to the construction of a multi-partite graph composed of three types of nodes, each representing distinct semantic granularities: (1) *Chunk*, (2) *knowledge Unit*, and (3) *Entity*. These nodes are connected through extraction and containment relations, forming a coherent multi-partite graph, as detailed in Section 3.2 and illustrated in Figure 3.

Intuitively, each sentence in a text chunk can serve as a basic knowledge unit, and lightweight NLP tools [4] can be used to extract these units. However, this approach overlooks sentence context, leading to contextual ambiguity – semantically similar sentences from different chunks may actually have distinct meanings. For example, as shown in Figure 2, two such sentences extracted by an NLP tool may have high cosine similarity (0.91) despite differing in meaning. To address this, we leverage LLMs to incorporate context when extracting knowledge units. As a result, the LLM-extracted units in the same example show much lower similarity (0.51), effectively capturing context-sensitive distinctions. Clearly, directly using LLMs to extract the units for all text chunks is very time and money-consuming. In this paper, we propose a novel hybrid extraction strategy that combines the advantages of powerful LLMs with lightweight NLP tools [4]. An ideal strategy would involve an oracle model that can identify which knowledge unit in a chunk may exhibit contextual ambiguity with units in other chunks. When such ambiguity is detected, we can use LLMs to resolve it, while relying on NLP tools for unambiguous units—thereby optimizing both efficiency and accuracy. Although such an oracle model does not exist, we can use semantic similarity between chunks as a proxy to evaluate potential contextual ambiguity, since knowledge units

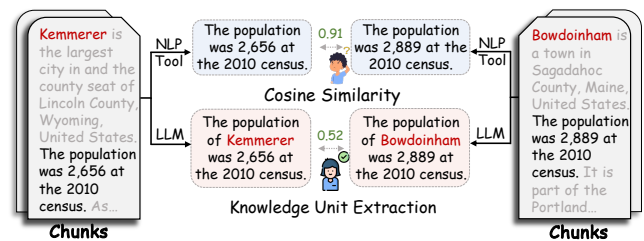


Figure 2: Comparison between sentence-level and LLM-extracted knowledge units. While the sentence-level units (top) lack specificity, the LLM-extracted units (bottom) offer more precise and complete semantic representations.

in highly similar chunks are intuitively more prone to ambiguity. To address this, we assign chunks with high semantic similarity to others for LLMs processing, while the remainder use NLP tools. To balance token cost and extraction accuracy, we formulate the chunk assignment as a 0-1 knapsack problem [33], aiming to maximize the total semantic similarity of the chunks selected for LLM processing within a given token budget. This strategy matches the performance of end-to-end LLM-based unit extraction, but uses only 50% of the tokens (see Experiment 4.3). Remarkably, CUE-RAG matches or outperforms baselines even without using an LLM for indexing (see Experiment 4.2).

To address **Limitation 2**, we propose *Query-driven iterative retrieval (Q-Iter)*, an iterative retrieval strategy that alternately traverses knowledge units and entities. The process begins by extracting entities from the input query to activate related entities, while concurrently using semantic search to anchor associated knowledge units. These units, in turn, expand the entity set by introducing entities referenced in their content. The strategy then performs constrained multihop traversal over the multi-partite graph to retrieve more relevant units. To ensure alignment with the query, each candidate unit is scored using a lightweight re-ranker specialized in query-context relevance. Finally, the collected knowledge units are mapped to their originating text chunks, which are subsequently re-ranked to yield the final context for answer generation.

In our experiments, we evaluate 13 solutions across three datasets, focusing on two key aspects: (1) *Cost efficiency*, based on token usage during offline indexing and online retrieval; and (2) *QA performance*, measured by F1 score and Accuracy. Remarkably, CUE-RAG demonstrates significant improvements over the SOTA baselines, delivering up to 99.33% higher Accuracy and 113.51% greater F1 score while simultaneously reducing indexing costs by 72.58%. Remarkably, the zero-token variant of CUE-RAG achieves comparable or superior performance to baselines. This highlights CUE-RAG’s superior graph indexing and inherent retrieval capabilities.

In summary, we make the following contributions through the development and evaluation of CUE-RAG:

- We propose a multi-partite graph index that integrates text chunks, knowledge units, and entities to support semantically coherent retrieval across multiple levels of granularity.

- We propose a hybrid strategy for knowledge unit extraction that maximizes LLM processing benefits while minimizing token usage.
- We propose Q-Iter, an iterative retrieval strategy that incrementally expands relevant knowledge units through semantic search and constrained graph traversal, significantly improving RAG performance.
- We empirically validate the effectiveness of CUE-RAG and the proposed retrieval strategy through comprehensive experiments against competitive baselines.

## 2 Preliminary

### 2.1 Terminology

Let  $\mathcal{T}$  be a text corpora whose element  $t_i \in \mathcal{T}$  is a text chunk of token length  $\leq l$ . The embedding of each text chunk  $t_i$  is defined as  $\phi(t_i)$ . We define a graph as  $\mathcal{G} = (\mathcal{V}, \mathcal{E})$ , where  $\mathcal{V}$  represents the set of nodes, and  $\mathcal{E} \subseteq \mathcal{V} \times \mathcal{V}$  denotes the set of edges connecting pairs of nodes. In addition, we use calligraphic uppercase letters (e.g.,  $\mathcal{S}$ ) to represent a set of elements. Table 1 provides a summary of commonly used notations.

**Table 1: Notations and meanings.**

Category	Notation	Meaning
Text	$\mathcal{R}(\cdot, \cdot)$	The re-ranking function
	$\phi(t_i)$	The embedding of text $t_i$
Processing	$\oplus(\mathcal{S})$	Concatenation of texts in set $\mathcal{S}$
	$\mathcal{T}, t_i, l$	Text $t_i \in \mathcal{T}$ whose length is $\leq l$
Retrieval	$M$	Beam size $M$
	$D$	Search depth $D$
	$N$	Returned chunks size $N$
	$K$	Top- $K$ relevant results $K$
	$\alpha$	Token constraint coefficient $\alpha$
Index	$\mathcal{G} = (\mathcal{V}, \mathcal{E})$	Edges set $\mathcal{E}_e \subseteq \mathcal{V}_e \times \mathcal{V}_{\mathcal{K}}$
	$\mathcal{E} = \mathcal{E}_c \cup \mathcal{E}_e$	Entity nodes set $\mathcal{V}_e$
	$\mathcal{V} = \mathcal{V}_{\mathcal{T}} \cup \mathcal{V}_{\mathcal{K}} \cup \mathcal{V}_e$	Chunk nodes set $\mathcal{V}_{\mathcal{T}}$
		Knowledge unit nodes set $\mathcal{V}_{\mathcal{K}}$

### 2.2 Background

Representative graph-based RAG methods typically follow two key stages: offline indexing and online retrieval. In the offline phase, a KG  $\mathcal{G}$  is constructed from a text corpora  $\mathcal{T}$  by extracting salient components, including nodes and edges, together with their associated textual attributes, such as descriptions or keywords [8, 13]. These components are then stored in vector databases or graph systems for efficient retrieval [25, 26]. During online retrieval, the input query  $q$  is usually incorporated only at the initial step, using its semantic embedding or extracted entities to match nodes or relations in  $\mathcal{G}$  [8, 13–15, 20, 38]. Then a subgraph is retrieved by expanding the local neighborhood of these seed nodes or relations. The structured subgraph and its associated content are incorporated into a prompt template to support LLM-based answer generation. However, as discussed in Section 1, existing methods exhibit two key limitations. First, the constructed KG is incomplete, which affects its effectiveness in supporting accurate answer generation.

Second, they suffer from semantic misalignment due to limited query integration during retrieval and heavy reliance on LLMs for iterative query reformulation.

## 3 Our Proposed Approach: CUE-RAG

**Our Goals.** The objective of this work is to improve the effectiveness of graph-based RAG by addressing the limitations in existing methods. Specifically, we aim to: (1) design a multi-partite graph index that supports semantically coherent retrieval across multiple levels of granularity; (2) develop a hybrid strategy for knowledge unit extraction that balances LLM utility with computational cost; and (3) propose Q-Iter, an iterative retrieval strategy that improves retrieval accuracy.

We provide an overview of CUE-RAG in Section 3.1 and CUE-RAG’s architecture, comprising two core modules: CUE-Index for offline indexing in Section 3.2 and Q-Iter for online retrieval in Section 3.3.

### 3.1 Overview

At a high level, CUE-RAG consists of two modules: offline indexing CUE-Index and online retrieval Q-Iter. As shown in Figure 3, offline CUE-Index has two stages:

- (1) Multi-Partite Graph Construction: Algorithm 1 constructs a multi-partite graph  $\mathcal{G} = (\mathcal{V}, \mathcal{E})$  by linking chunk nodes to their corresponding knowledge unit nodes, and knowledge unit nodes to the entities they reference. This three-tier structure enables semantically coherent retrieval across multiple levels of granularity.
- (2) Hybrid Extraction: Given a text corpora  $\mathcal{T}$  and a token constraint coefficient  $\alpha \in [0, 1]$ , a subset of core text chunks  $\mathcal{T}_c \in \mathcal{T}$  is selected based on relevance metrics. For  $t \in \mathcal{T}_c$ , LLM is employed to extract disambiguated knowledge units. For  $t \in \mathcal{T} \setminus \mathcal{T}_c$ , NLP tool segments the text into sentence-level units. Finally, entities are extracted from all resulting knowledge units using NLP tool.

During online retrieval, Q-Iter begins by extracting entities from the input query  $q$  to activate related entities, while semantic search anchors initial knowledge units. These units expand the entity set via referenced entities, enabling constrained multihop traversal over  $\mathcal{G}$  to retrieve additional relevant units. The resulting units are mapped to their source chunks and re-ranked to form the final context for answer generation.

### 3.2 Offline CUE-Index

**Multi-Partite Graph Construction.** CUE-Index constructs a multi-partite graph  $\mathcal{G}$  from a text corpora  $\mathcal{T}$ , organizing information across three semantic levels, as illustrated in Figure 3. In the upper layer, chunk nodes  $\mathcal{V}_{\mathcal{T}}$  represent coarse-grained content by encoding text chunks. The intermediate layer contains knowledge unit nodes  $\mathcal{V}_{\mathcal{K}}$ , which capture semantically richer information distilled from the text. In the lower layer, entity nodes  $\mathcal{V}_e$  encode fine-grained factual elements extracted from knowledge units. The graph is then connected by two types of edges:  $\mathcal{E}_c$ , linking each chunk node to its corresponding knowledge units, and  $\mathcal{E}_e$ , connecting knowledge units to the entities they mention.

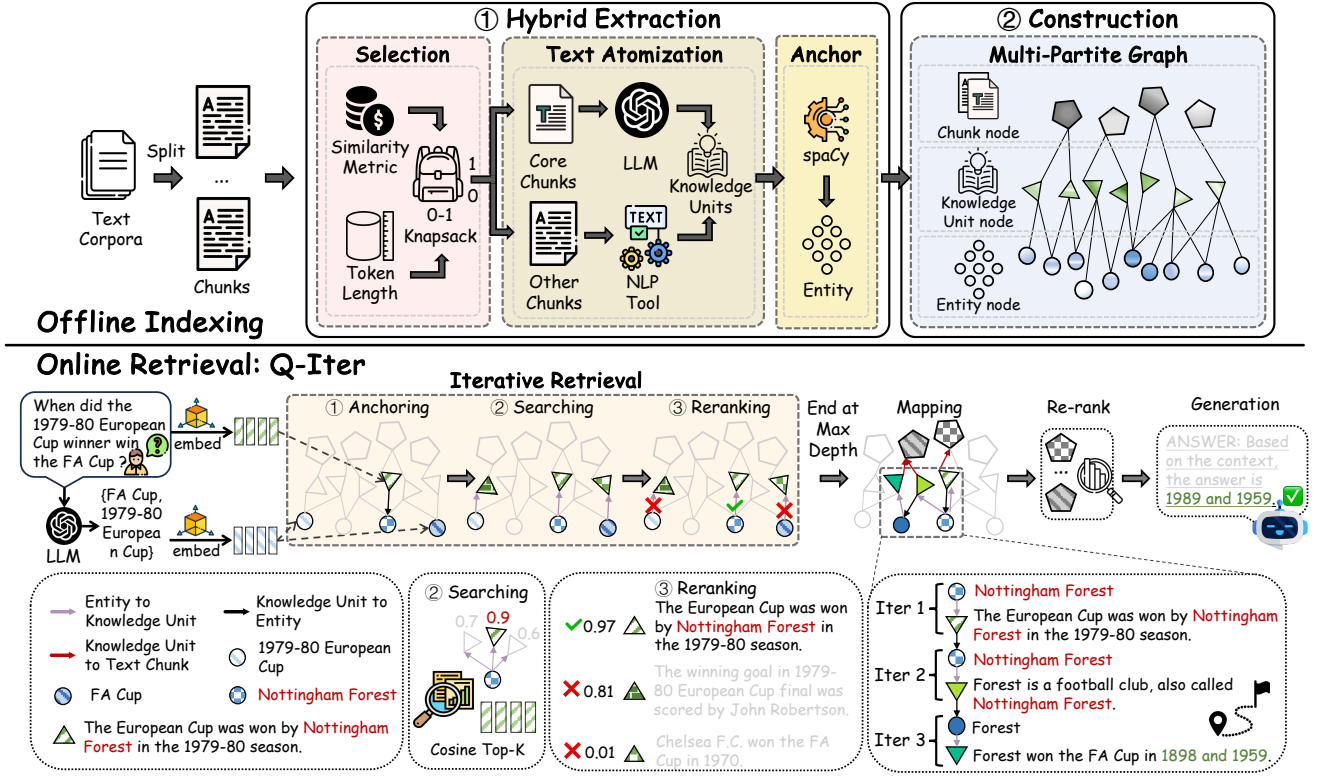


Figure 3: CUE-RAG consists of two phases: offline indexing and online retrieval.

**Hybrid Extraction.** As shown in Algorithm 1, the hybrid extraction process begins by selecting a subset of core text chunks  $\mathcal{T}_c \subseteq \mathcal{T}$  using Algorithm 2, based on a token constraint coefficient  $\alpha \in [0, 1]$ . Algorithm 2 formulates the selection stage as a 0-1 knapsack problem, where each chunk is assigned a value based on its relevance score and a weight corresponding to its token length, selecting the subset that maximizes relevance under the token budget. In Algorithm 1, once  $\mathcal{T}_c$  is identified (Line 3), each text chunk  $t_i$  is processed according to its selection status (Lines 6–11). For  $t_i \in \mathcal{T}_c$ , a LLM extracts disambiguated knowledge units  $\mathcal{K}_i$  that capture core semantics. For  $t_i \in \mathcal{T} \setminus \mathcal{T}_c$ , lightweight NLP tools [4] segment the text into sentences as knowledge units  $\mathcal{K}_i$  to ensure broad coverage at lower computational cost. All text chunks and extracted knowledge units are instantiated as text nodes  $\mathcal{V}_{\mathcal{T}}$  and knowledge unit nodes  $\mathcal{V}_{\mathcal{K}}$ , respectively, forming the upper and intermediate layers of the multi-partite graph. Finally, in Lines 12-13, the Named Entity Recognition (NER) component in spaCy [17] is utilized to extract entities  $\mathcal{V}_k$  for each knowledge unit  $k$ . All these extracted entities  $\mathcal{V}_k$  are collected and form entity nodes  $\mathcal{V}_e$ , acting as anchors for precise information retrieval.

### 3.3 Online Q-Iter

In Algorithm 3, Q-Iter takes as input a query  $q$  and a multi-partite graph index  $\mathcal{G}$ . The retrieval process operates under four parameters: the number of most relevant results  $K$ , maximum search depth

#### Algorithm 1: CUE-Index $(\mathcal{T}, \alpha)$

- 1 **Input:** Text corpora  $\mathcal{T} = \{t_1, \dots, t_n\}$ , constraint  $\alpha \in [0, 1]$
- 2 **Output:** A hierarchical graph index  $\mathcal{G} = (\mathcal{V}, \mathcal{E})$
- 3  $\mathcal{T}_c \leftarrow \text{Chunk-Selection}(\mathcal{T}, \alpha)$  in Algorithm 2;
- 4  $\mathcal{V}_{\mathcal{T}} \leftarrow \{t_i \mid t_i \in \mathcal{T}\}$ ,  $\mathcal{V}_{\mathcal{K}} \leftarrow \emptyset$ ,  $\mathcal{V}_e \leftarrow \emptyset$ ;
- 5  $\mathcal{E}_c \leftarrow \emptyset$ ,  $\mathcal{E}_e \leftarrow \emptyset$ ;
- 6 **foreach**  $t_i \in \mathcal{V}_{\mathcal{T}}$  **do**
- 7     **if**  $t_i \in \mathcal{T}_c$  **then**
- 8          $\mathcal{K}_i \leftarrow$  extracted by LLM from  $t_i$ ;
- 9     **else**
- 10          $\mathcal{K}_i \leftarrow$  split by NLP tool from  $t_i$ ;
- 11      $\mathcal{V}_{\mathcal{K}} \leftarrow \mathcal{V}_{\mathcal{K}} \cup \mathcal{K}_i$ ;  $\mathcal{E}_c \leftarrow \mathcal{E}_c \cup \{(t_i, k) \mid k \in \mathcal{K}_i\}$ ;
- 12 **foreach**  $k \in \mathcal{V}_{\mathcal{K}}$  **do**
- 13      $\mathcal{V}_k \leftarrow \text{NER}(k)$ ;  $\mathcal{V}_e \leftarrow \mathcal{V}_e \cup \mathcal{V}_k$ ;
- 14      $\mathcal{E}_e \leftarrow \mathcal{E}_e \cup \{(v, k) \mid v \in \mathcal{V}_k\}$ ;
- 15 **return**  $\mathcal{G} = (\mathcal{V}_{\mathcal{T}} \cup \mathcal{V}_{\mathcal{K}} \cup \mathcal{V}_e, \mathcal{E}_c \cup \mathcal{E}_e)$ ;

$D$ , beam size  $M$  per depth level, and returned chunks size  $N$ . Q-Iter proceeds through three carefully designed stages as follows: **Entity Anchoring.** Inspired by cognitive theories of spreading activation [1, 6], we first extract entities from the input query using LLM and identify their top- $K$  most similar entity nodes in  $\mathcal{G}$  to form the initial query set  $\mathcal{V}_q^{(0)}$ . In parallel, we retrieve the top- $K$

---

**Algorithm 2:** Chunk-Selection  $(\mathcal{T}, \alpha)$ 


---

```

1 Input: Text corpora  $\mathcal{T} = \{t_1, \dots, t_n\}$ , constraint  $\alpha \in [0, 1]$ 
2 Output: a core subset of text chunks  $\mathcal{T}_c \in \mathcal{T}$ 
3  $W_{\text{total}} \leftarrow 0, \mathcal{S} \leftarrow \emptyset;$ 
4 foreach  $t_i \in \mathcal{T}$  do
5    $w_i \leftarrow \text{TokenLength}(t_i);$ 
6    $v_i \leftarrow \text{BLEU}(t_i, \mathcal{T} \setminus \{t_i\});$   $\triangleright$  Standard BLEU calculation
7    $W_{\text{total}} \leftarrow W_{\text{total}} + w_i; \mathcal{S} \leftarrow \mathcal{S} \cup \{(w_i, v_i)\};$ 
8  $W_{\text{max}} \leftarrow \lceil \alpha \cdot W_{\text{total}} \rceil;$ 
9  $\mathcal{T}_c \leftarrow \text{Knapsack}(\mathcal{S}, W_{\text{max}});$ 
10 return  $\mathcal{T}_c;$ 

```

---

knowledge units that are most semantically similar to the query and expand  $\mathcal{V}_q^{(0)}$  by including all entities referenced in these units. This dual expansion incorporates both directly matched entities and entities introduced via semantically aligned knowledge units, enhancing the coverage and specificity of subsequent multihop retrieval. We refer to this combined process of Spreading Activation and Knowledge Anchoring as `Entity-Anchoring`, which yields the initial seed nodes  $\mathcal{V}_q^{(0)}$ . Due to space constraints, the full pseudocode is deferred to Appendix A.

**Iterative Retrieval.** The algorithm 3 takes the seed nodes  $\mathcal{V}_q^{(0)}$  as input. In Line 5, it initializes  $Q^{(0)}$  with tuples  $(v, \phi(q), \emptyset)$  for each anchor  $v \in \mathcal{V}_q^{(0)}$ , where  $\phi(q)$  is the query embedding and  $\emptyset$  will accumulate the retrieved knowledge units. For each depth  $d$  from 1 to  $D$ , it processes the query queue  $Q^{(d-1)}$  in Lines 6-18. In Lines 8-9, for each  $(v, \phi_v, \mathcal{S}_v) \in Q^{(d-1)}$ , the algorithm retrieves top- $K$  new knowledge units  $\mathcal{K}_v \subseteq \mathcal{V}_{\mathcal{K}} \setminus \mathcal{S}_v$  using  $\phi_v$ , ensuring relevance while avoiding redundancy. In Lines 10-15, for each  $k \in \mathcal{K}_v$ , the algorithm first updates the query embedding by subtracting  $k$ 's embedding, dynamically shifting focus to uncovered information and avoiding redundancy (see Experiment 4.4). Next, the algorithm adds  $k$  to  $\mathcal{S}_v$ , sorts it canonically, then uses re-ranker  $\mathcal{R}$  to score  $\oplus(\mathcal{S}'_v)$  for coherence with query  $q$ . Unlike semantic similarity measures,  $\mathcal{R}$  specializes in query-context relevance scoring, allowing a more accurate assessment of knowledge units' relevance to  $q$ . Then, the algorithm: (1) finds adjacent entities  $\mathcal{V}'$  via  $k$ 's edges as next-depth anchors, and (2) updates  $C$  with the new state tuple and its re-ranked  $score$ . Finally, in Lines 16-18, the algorithm prunes  $C$  to the top- $M$  tuples  $C'$  based on their re-ranked  $scores$ , merges them into  $C^*$ , and initializes  $Q^{(d)}$  for the next iteration.

**Final Re-ranking.** In Lines 19-23, the algorithm retrieves text nodes  $\mathcal{T}'$  citing  $\mathcal{S}$  via  $\mathcal{E}_c$ , then selects top- $N$  by their re-ranked  $scores$  to form final chunks  $\mathcal{T}^*$  for augmented generation.

## 4 Experiments

In this section, we assess the effectiveness of CUE-RAG by addressing the following research questions:

- **Q1:** How does CUE-RAG compare to existing baselines in terms of QA performance and cost efficiency?
- **Q2:** How does our hybrid extraction strategy compare to alternatives and full LLM-based extraction in terms of QA performance and cost efficiency?

---

**Algorithm 3:** Q-Iter  $(q, \mathcal{G}, K, D, M, N)$ 


---

```

1 Input: query  $q$ , hierarchical graph index
    $\mathcal{G} = (\mathcal{V}_{\mathcal{T}} \cup \mathcal{V}_{\mathcal{K}} \cup \mathcal{V}_e, \mathcal{E}_c \cup \mathcal{E}_e)$ , number of most relevant
   results  $K$ , search depth  $D$ , beam size  $M$  per depth, returned
   candidate chunks size  $N$ 
2 Output: top- $N$  relevant chunks  $\mathcal{T}^*$ 
3  $\mathcal{V}_q^{(0)} \leftarrow \text{Entity-Anchoring}(q, \mathcal{G}, K)$  in Algorithm 4;
4 # Iterative Retrieval
5  $Q^{(0)} \leftarrow \{(v, \phi(q), \emptyset) \mid v \in \mathcal{V}_q^{(0)}\}; C^* \leftarrow \emptyset;$ 
6 foreach  $d = 1, \dots, D$  do
7    $C \leftarrow \emptyset;$ 
8   foreach  $(v, \phi_v, \mathcal{S}_v) \in Q^{(d-1)}$  do
9      $\mathcal{K}_v \leftarrow \arg \max_{k \in \mathcal{V}_{\mathcal{K}} \setminus \mathcal{S}_v \wedge (v, k) \in \mathcal{E}_e \wedge |\mathcal{K}_v| = K} \cos(\phi(k), \phi_v)$ 
10    foreach  $k \in \mathcal{K}_v$  do
11       $\phi'_v \leftarrow \phi_v - \phi(k)$   $\triangleright$  Update query embedding
12       $\mathcal{S}'_v \leftarrow \text{sort}(\mathcal{S}_v \cup \{k\})$   $\triangleright$  Dictionary sorting
13       $score \leftarrow \mathcal{R}(q, \oplus(\mathcal{S}'_v))$   $\triangleright$  Re-rank
14       $\mathcal{V}' \leftarrow \{v \mid (v, k) \in \mathcal{E}_e\}$ 
15       $C \leftarrow C \cup \{(\mathcal{V}', \phi'_v, \mathcal{S}'_v, score)\}$ 
16     $C' \leftarrow \arg \max_{(\mathcal{V}, \phi, \mathcal{S}, score) \in C \wedge |C'| = M} score$   $\triangleright$  Pruning
17     $C^* \leftarrow C^* \cup C'$ 
18     $Q^{(d)} \leftarrow \bigcup_{(\mathcal{V}, \phi, \mathcal{S}, score) \in C'} \{(v, \phi, \mathcal{S}) \mid v \in \mathcal{V}\}$ 
19 # Final Re-ranking
20  $\mathcal{T}' \leftarrow \emptyset$ 
21 foreach  $(\mathcal{V}, \phi, \mathcal{S}, score) \in C^*$  do
22    $\mathcal{T}' \leftarrow \mathcal{T}' \cup \{t \mid k \in \mathcal{S} \wedge (t, k) \in \mathcal{E}_c\}$ 
23  $\mathcal{T}^* \leftarrow \arg \max_{t \in \mathcal{T}' \wedge |\mathcal{T}^*| = N} \mathcal{R}(q, t)$ 
24 return  $\mathcal{T}^*$ 

```

---

- **Q3:** How does each stage of online retrieval Q-Iter contribute to the overall performance?
- **Q4:** How sensitive is CUE-RAG to variations in hyperparameter settings?

All experiments are conducted on a Linux machine with an Intel Xeon 2.0 GHz CPU, 1024 GB of memory, and 8 NVIDIA GeForce RTX A5000 GPUs (each with 24 GB of memory), capable of running both LLaMA3.0-8B [12] and Qwen2.5-32B [3] LLM models.

### 4.1 Experimental Setup

**Datasets.** We evaluate CUE-RAG's capability primarily on three multihop QA benchmarks, MuSiQue [37], HotpotQA [43], and 2WikiMultiHopQA (2Wiki. below) [16] dataset, all of which are extensively utilized within the QA and graph-based RAG research communities. Following prior work [14, 31, 36, 45], we extract 1,000 questions from each validation set, while the corresponding paragraphs for all sampled instances are preprocessed into a unified text corpora  $\mathcal{T}$ , maintaining question-paragraph alignment for evaluation. The details of these datasets are shown in Appendix Table 5.

**Metrics.** We primarily evaluate each solution’s performance along two dimensions: QA performance and cost efficiency. For QA performance, we report Accuracy (Acc. below) and F1 score (F1 below), where Acc. measures whether the golden answers are included in the generation answer rather than requiring exact match [2, 23], and F1 is computed via token-level overlap between golden and generated answers, balancing precision and recall to assess both answer completeness and correctness [14, 45]. For cost efficiency, we quantify two metrics: total token expenditure for offline indexing and average token consumption per online query.

**Baselines.** We evaluate the performance of 13 solutions categorized as follows:

- **Simple Baselines:** We consider two straightforward approaches: (1) the Zero-shot method, which directly applies an LLM for question answering without any retrieval, and (2) VanillaRAG, which retrieves relevant passages through query embedding similarity before using these passages as context for LLM answer generation.
- **Graph-Structured Baselines:** We evaluate six graph-structured baselines that construct text-attribute KG using LLMs for content retrieval: HippoRAG [14], KETRAG [20], and local search of GraphRAG (LGraphRAG) [8] and three versions of LightRAG (LLightRAG for local search, GLightRAG for global search, and HLightRAG for hybrid search) [13], excluding GraphRAG’s global version as it targets abstract QA rather than specific multi-hop queries.
- **Tree-Structured Baselines:** We evaluate two tree-based baselines: RAPTOR [34] (using semantic similarity) and SIRERAG [45] (combining semantic and lexical similarity), both constructing multi-level trees for passage organization and retrieval.
- **Our proposed solutions:** Our approach supports three operational modes, determined by a hyperparameter  $\alpha \in [0, 1]$ , which controls the proportion of tokens in  $\mathcal{T}$  processed by LLMs during offline indexing. CUE-RAG-0.0 ( $\alpha = 0.0$ ) demonstrates the strong performance of our LLM-free graph index and retrieval strategy. CUE-RAG-0.5 ( $\alpha = 0.5$ ) highlights the effectiveness of our hybrid extraction strategy, achieving strong performance while reducing 50% indexing cost. CUE-RAG-1.0 ( $\alpha = 1.0$ ) represents the full-capacity configuration, where all text chunks are processed by LLMs, enabling the system to achieve SOTA performance.

**Settings.** To ensure a fair comparison, all methods are implemented within a unified framework and environment [48]. During the LLM generation phase, we employ a strategy by duplicating the input query to the end of the original prompt. This design explicitly mitigates the “lost in the middle” effect [22] observed in approaches like LightRAG, where placing the question before lengthy context can cause the model to overlook the task objective [22, 32]. Furthermore, inspired by the prompt designs of SIRERAG [45] and KETRAG [20], which include phrases like “Answer this question as short as possible” to prevent verbose or irrelevant outputs, we uniformly add this instruction to the final prompt of each method. This ensures concise responses, maintaining evaluation fairness and highlighting our method’s effectiveness. For other hyperparameters of each method, we follow the original settings in their available codes. For NLP pre-processing, we employ the following tools: cl100k\_base from tiktoken library [28] for word tokenization and counting, NLTK’s

sent\_tokenize [4] for sentence segmentation, and spaCy [17] for named entity recognition. For LLM inference, we use LLaMA3.0-8B [12] and Qwen2.5-32B [3], with a maximum token limit of 8,000. In top- $K$  selection tasks, we set  $K = 5$  to accommodate token constraints. The embedding model for vector search is BGE-M3 [5], while re-ranking is performed using the lightweight yet powerful BGE-Reranker-v2-M3 [5]. As for our proposed approach, CUE-RAG employs the following default configurations: the number of most relevant results  $K$  is set to 3, search depth  $D$  to 3, beam size  $M$  per depth to 5, and returned candidate chunks  $N$  to 5, ensuring that all methods ultimately retrieve the same number of query-relevant chunks (i.e., 5) for fair comparison. By default, we set the value of  $\alpha$  to 1 if it is not explicitly specified. Additionally, BLEU score [29] serves as the core selection metric for relevance scoring.

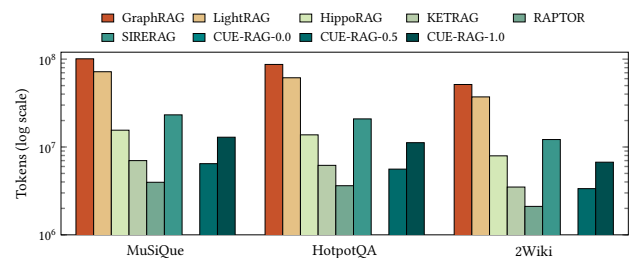


**Figure 4: Token cost comparison during offline indexing using LLaMA3.0-8B. Reported costs include prompt and completion tokens for offline indexing. The seventh bar is empty because CUE-RAG-0.0 requires no LLM usage during indexing.**

## 4.2 Performance Evaluation (Q1)

In the first set of experiments, we evaluate the QA performance and cost efficiency of CUE-RAG against ten existing solutions under three configurations:  $\alpha$  equal to 0.0, 0.5, and 1.0, representing no LLM usage for indexing, selective LLM-aided indexing, and full LLM processing for indexing, respectively.

As shown in Table 2, CUE-RAG consistently achieves superior generation quality across multiple benchmark datasets when evaluated with different LLMs, with CUE-RAG-1.0 establishing SOTA performance in both average F1 and Acc. Specifically, it outperforms the strong baseline KETRAG by 21.53% in average F1, achieving up to a 73.15% improvement on the MuSiQue dataset when using Qwen2.5-32B, while also surpassing another competitive baseline SIRERAG by 5.75% in average Acc., with gains reaching up to 15.49% on the 2Wiki dataset when using LLaMA3.0-8B. Remarkably, CUE-RAG-0.5 demonstrates competitive QA performance and cost efficiency relative to KETRAG. It achieves improvements of 19.29%/27.19% in average F1/Acc., along with up to 74.00%/99.33% improvements in F1/Acc., respectively. Concurrently, it reduces token costs by up to 9.41%/83.87% during offline indexing and online querying shown in Figure 4 and 5. Notably, CUE-RAG-0.0, which entirely avoids LLM usage in indexing, still matches or exceeds the capabilities of SIRERAG and KETRAG. Compared to KETRAG, it improves average F1/Acc. by 13.01%/21.86% and F1/Acc. by up to 62.52%/89.65%, while reducing token costs by 100%/82.92% during offline indexing and online querying. Against SIRERAG, it achieves

**Table 2: Overall Performance of RAG Solutions. The best and second-best results among the ten competitor solutions (excluding the CUE-RAG series) in each column are highlighted in bold and underlined, respectively.**

Method	LLaMA3.0-8B						Qwen2.5-32B						Avg	
	MuSiQue		HotpotQA		2Wiki		MuSiQue		HotpotQA		2Wiki			
	F1	Acc.												
<b>Simple Baselines</b>														
Zero-shot	7.14	5.11	24.34	25.30	18.88	33.78	9.62	5.71	25.51	25.90	26.44	27.10	18.66	20.48
Vanilla	12.28	14.21	40.62	52.50	18.22	34.00	20.97	21.02	53.55	60.50	30.94	44.80	29.43	37.84
<b>Graph-Structured Baselines</b>														
LGraphRAG	9.23	14.21	24.81	43.90	15.11	42.20	13.12	19.12	34.04	53.20	21.57	46.20	19.65	36.47
LLightRAG	7.94	6.91	25.43	36.30	17.35	33.60	13.82	18.52	34.09	49.10	22.53	48.40	20.19	32.14
GLightRAG	5.34	5.14	17.80	27.40	11.82	23.20	9.31	11.51	21.69	34.30	8.09	35.70	12.34	22.88
HLightRAG	7.87	9.41	25.82	37.40	13.16	28.40	14.57	22.62	35.89	55.60	19.16	52.30	19.41	34.29
HippoRAG	11.58	11.81	39.63	44.40	24.94	<u>48.20</u>	15.00	20.42	40.36	52.20	26.95	53.70	26.41	38.46
KETRAG	<u>16.25</u>	12.51	<u>48.75</u>	47.10	<u>27.90</u>	41.40	21.08	16.52	<u>61.94</u>	57.70	<u>50.02</u>	49.90	<u>37.66</u>	37.52
<b>Tree-Structured Baselines</b>														
RAPTOR	10.58	16.22	34.18	<u>56.50</u>	16.92	43.30	17.31	21.12	47.09	63.70	28.88	47.20	25.83	41.34
SIRERAG	11.99	<u>21.22</u>	34.02	55.70	18.34	43.90	<u>22.46</u>	<u>31.93</u>	46.75	<b>65.10</b>	33.88	<u>57.10</u>	27.91	<u>45.83</u>
CUE-RAG-0.0	24.10	21.02	53.18	57.20	32.19	46.60	34.26	31.33	62.14	63.50	49.47	54.70	42.56	45.73
CUE-RAG-0.5	<b>25.60</b>	22.12	55.80	<b>59.50</b>	35.52	48.90	<b>36.68</b>	<b>32.93</b>	63.44	64.10	52.49	58.80	44.92	47.73
CUE-RAG-1.0	25.48	<b>22.32</b>	<b>55.97</b>	59.20	<b>37.41</b>	<b>50.70</b>	36.50	32.83	<b>64.02</b>	<u>64.70</u>	<b>55.20</b>	<b>61.00</b>	<b>45.76</b>	<b>48.46</b>

52.50% higher average F1 and up to 101% improvement in F1, alongside 100%/56.06% reductions in indexing and querying costs.

Beyond outperforming the two strong baselines (KETRAG and SIRERAG), CUE-RAG demonstrates superior QA performance across all evaluated datasets when compared with other eight alternatives. This consistent advantage highlights the effectiveness of its innovative indexing and retrieval strategies in multi-hop QA scenery.

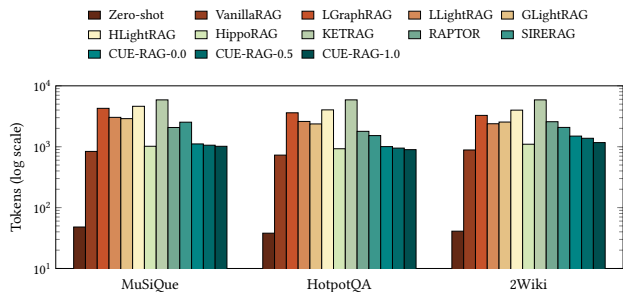


**Figure 5: Token cost comparison per query during online retrieval with LLaMA3.0-8B. Reported costs include prompt and completion tokens for answer generation. For methods involving additional LLM-based query processing (e.g., keyword or entity extraction), such preprocessing costs are also included where applicable.**

### 4.3 Effectiveness of Hybrid Extraction (Q2)

This set of experiments evaluates the effectiveness of our hybrid extraction strategy for knowledge units, as described in Section 3.2.

Table 3 reports the QA performance of four methods, each constrained to use only 50% of the total token budget for LLM processing ( $\alpha = 0.5$ ). The methods differ in their chunk selection strategies: RANDOM (random selection), COS (our Chunk-Selection using cosine similarity), and BLEU (our Chunk-Selection using BLEU score). For direct comparison, we also include the performance of CUE-RAG-1.0 (BLEU), which uses 100% of the token budget. Results show that both COS and BLEU significantly outperform RANDOM across average F1 and Acc. Among them, the BLEU-based strategy achieves the highest performance, exceeding RANDOM and COS by 3.14% and 0.46% in average F1, and by 3.05% and 0.21% in average Acc, respectively. These gains underscore the effectiveness of our hybrid extraction approach in the offline indexing stage.

While CUE-RAG-1.0 (BLEU) generally yields stronger results, CUE-RAG-0.5 (BLEU) achieves 94.95%–100.51% of its performance, with half the token usage. A particularly interesting phenomenon emerges on the MuSiQue dataset with LLaMA3.0-8B and Qwen2.5-32B, where CUE-RAG-0.5 (BLEU) occasionally outperforms its full-token counterpart. This suggests that certain questions in MuSiQue exhibit a stronger lexical alignment with original corpus sentences than with LLM-extracted knowledge units, as the paraphrasing process may substitute critical terms with less relevant alternatives. Overall, these results demonstrate that our hybrid extraction strategy can maintain robust QA performance while significantly optimizing token efficiency during indexing.

### 4.4 Ablation Study (Q3)

This experiment demonstrates the role of the first two stages, Spreading Activation (SA, below) and Knowledge Anchoring (KA,

**Table 3: Performance comparison of CUE-RAG-0.5 using different core chunk selection strategies. The table highlights the best and second-best results in each column with bold and underlined formatting, respectively.**

Method	LLaMA3.0-8B						Qwen2.5-32B						Avg	
	MuSiQue		HotpotQA		2Wiki		MuSiQue		HotpotQA		2Wiki			
	F1	Acc.												
CUE-RAG-0.5 (RANDOM)	<u>25.18</u>	21.32	54.44	57.60	34.00	46.90	<u>36.61</u>	<b>33.93</b>	61.59	63.40	49.49	54.70	43.55	46.31
CUE-RAG-0.5 (COS)	24.64	<u>21.42</u>	<u>55.80</u>	<u>59.10</u>	<u>35.18</u>	<b>49.10</b>	36.19	32.13	<b>63.65</b>	<b>64.90</b>	<b>52.83</b>	<b>59.10</b>	<u>44.72</u>	<u>47.63</u>
CUE-RAG-0.5 (BLEU)	<b>25.60</b>	<b>22.12</b>	<u>55.80</u>	<b>59.50</b>	<b>35.52</b>	<u>48.90</u>	<b>36.68</b>	<u>32.93</u>	<u>63.44</u>	<u>64.10</u>	<u>52.49</u>	<u>58.80</u>	<b>44.92</b>	<b>47.73</b>
CUE-RAG-1.0 (BLEU)	25.48	22.32	55.97	59.20	37.41	50.70	36.50	32.83	64.02	64.70	55.20	61.00	45.76	48.46

**Table 4: Ablation study of CUE-RAG-1.0, evaluating the contributions of key components: Knowledge Anchoring (KA.), Spreading Activation (SA.), and Query Updating (QU.). The best performance for each metric is highlighted in bold, while the second-best result is underlined.**

Method	LLaMA3.0-8B						Qwen2.5-32B						Avg	
	MuSiQue		HotpotQA		2Wiki		MuSiQue		HotpotQA		2Wiki			
	F1	Acc.												
CUE-RAG-1.0	<b>25.48</b>	<b>22.32</b>	<b>55.97</b>	<b>59.20</b>	<u>37.41</u>	<u>50.70</u>	<b>36.50</b>	<b>32.83</b>	<b>64.02</b>	<b>64.70</b>	<u>55.20</u>	<u>61.00</u>	<b>45.76</b>	<b>48.46</b>
w/o KA.	<u>25.26</u>	<u>22.02</u>	52.93	55.50	36.75	50.10	32.64	29.13	60.50	62.00	52.58	58.60	43.44	46.23
w/o SA.	23.18	19.52	53.48	55.70	34.76	45.60	31.64	28.03	59.12	59.90	48.57	55.70	41.79	44.08
w/o QU.	24.51	20.72	<u>54.51</u>	<u>56.80</u>	<b>38.00</b>	<b>51.50</b>	<u>35.36</u>	<u>32.03</u>	<u>62.52</u>	<u>64.10</u>	<b>55.27</b>	<b>61.80</b>	<u>45.03</u>	<u>47.83</u>
w/o QU. or KA.	22.53	18.82	52.00	53.90	36.52	49.50	31.93	28.33	60.14	62.00	52.72	58.90	42.64	45.24
w/o QU. or SA.	21.57	17.42	51.22	53.50	33.43	46.10	31.84	27.93	56.71	58.30	48.34	55.80	40.52	43.18

below) in Section 3.3 and the Query Updating (QU. below) in Iterative Retrieval, as Final Re-ranking is indispensable components of the overall search pipeline. Table 4 shows the performance of removing each mechanism, indicating that both contribute to the improvement of CUE-RAG’s retrieval capability. Specifically, Spreading Activation enhances the average F1 and Acc. by 9.5% and 9.95%, respectively, while Knowledge Anchoring provides improvement of 5.34% and 4.83%, and Query Updating improves the average F1 and Acc. by 1.63% and 1.32%. The superior performance of Spreading Activation can be attributed to its alignment in semantic granularity: the entities extracted from the query by the LLM are matched against entity nodes in the hierarchical graph, ensuring consistency. In contrast, Knowledge Anchoring relies on semantic embeddings of the query to align with knowledge unit nodes in the graph, which may introduce noise due to potential inconsistencies in semantic granularity. Query Updating improves F1 by up to 3.96% and Acc by 7.72% on MuSiQue, and by 2.68% and 4.23% on HotpotQA, but slightly degrades on 2Wiki. The performance decline on 2Wiki stems from its frequent semantically similar entities (e.g., familial relations or homonyms like Elizabeth I/II), which challenge disambiguation. Nevertheless, they collectively enhance the retrieval performance of CUE-RAG.

#### 4.5 Parameter Sensitivity (Q4)

In the final set of experiments, we analyze the sensitivity of our proposed approach using Qwen2.5-32B with respect to key hyperparameters: the number of top- $K$  retrieved results  $K$ , beam size  $M$ , search depth  $D$ , and token constraint coefficient  $\alpha$ . We evaluate  $K \in \{3, 5, 7, 9\}$ ,  $M \in \{3, 5, 7, 9\}$ ,  $D \in \{1, 2, 3, 4\}$ , and  $\alpha \in \{0, 0.25, 0.5, 0.75, 1.0\}$ .

First, as shown in Figure 6 (a), CUE-RAG does not exhibit a consistent improvement in generation quality with increasing  $K$  across all three datasets. Instead, the results suggest that  $K = 3$  provides sufficient retrieval results, while larger values introduce noise without meaningful gains. Next, Figure 6 (b) reveals that generation quality generally improves with larger beam sizes  $M$ . However, the gains plateau beyond  $M = 5$  or  $M = 7$ , and a slight decline occurs at  $M = 9$ . This indicates that  $M = 5$  strikes an optimal balance between generation quality and computational efficiency, as excessively large beam sizes may introduce noise with diminishing returns. Furthermore, Figure 6 (c) demonstrates that deeper search depth  $D$  leads to better performance, which aligns with the nature of the datasets, where most questions require 2 hops while fewer necessitate 3-4 hops. Nevertheless, when  $D = 4$ , generation quality slightly deteriorates, likely due to over-retrieval of irrelevant information for most 2-hops questions. Finally, Figure 6 (d) shows a positive correlation between the token constraint coefficient  $\alpha$  and generation quality. This is expected because higher

$\alpha$  values permit the LLM to process more chunks, thereby improving the quality of knowledge units and enhancing retrieval accuracy.

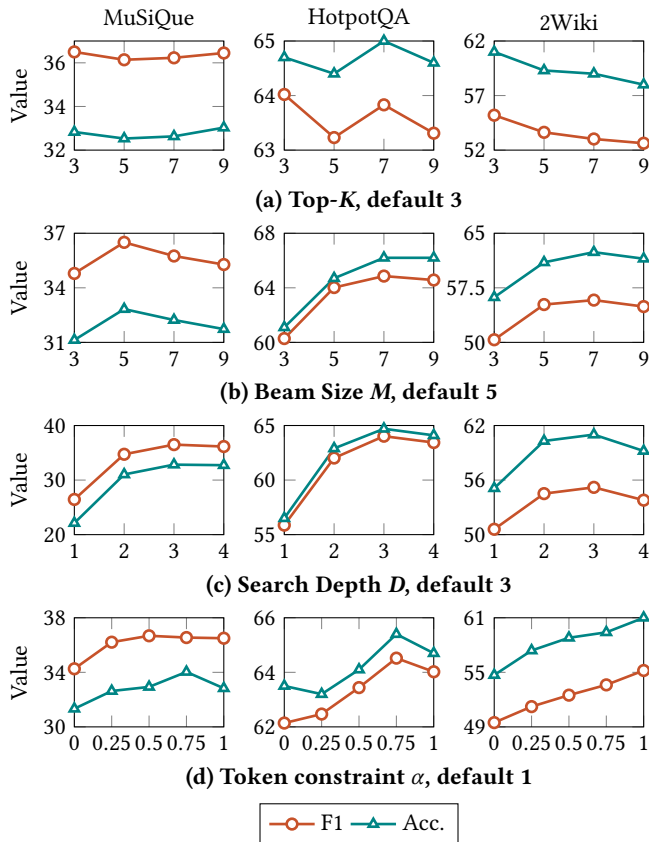


Figure 6: Performance analysis under different hyperparameter settings.

## 5 Related Works

We review some indexing and retrieval strategies in graph-based RAG methods. For a comprehensive discussion, we refer the reader to previous surveys [30, 46] and an in-depth analysis of graph-based RAG in a unified framework [48].

Among the early approaches, RAPTOR [34] introduces a bottom-up tree construction strategy. It begins with raw text chunks as leaf nodes, clusters their embeddings via Gaussian Mixture Models [24], then recursively summarizes clusters using LLMs and re-clusters them to build the tree bottom-up. During retrieval, all tree nodes are indexed in a vector database, enabling a fast semantic similarity search with query embeddings. Building on RAPTOR, SIRERAG [45] introduces a dual tree framework. It extracts propositions and entities from texts using LLMs, regrouping propositions linked to the same entity into new passages. These passages are then organized into a relatedness tree alongside the RAPTOR similarity tree, with both trees jointly indexed in the same vector database for retrieval. This hybrid approach aims to balance semantic similarity and relatedness coherence. Although these tree-based approaches demonstrate effective hierarchical organization, recent works have

explored graph-based alternatives for richer structural representation. Microsoft’s GraphRAG [8] first constructs a text-attributed KG by extracting entities, relationships, and other detailed contextual features from text fragments through LLMs. KG is then hierarchically clustered with the Leiden algorithm [35], and each cluster is summarized into a community report. For retrieval, the proposed local search retrieves relevant context from entities, relationships, community reports, and text chunks to augment response. LightRAG [13] constructs a KG from text chunks while using LLMs to augment both entities and relations with extracted keywords and leverages LLMs to extract query-relevant low-/high-level keywords for retrieval. It integrates local, global, and hybrid search strategies to fetch matching entities and relations, which are then combined with text chunks for answer generation. KETRAG [20] selects core text chunks based on their PageRank centrality in a KNN graph built using both semantic and lexical similarity. It then constructs a KG following Microsoft’s GraphRAG, though without community detection or report summarization, while organizing the remaining text chunks into a text-keyword bipartite graph. For retrieval, it adopts standard local search but innovates by extracting ego networks from both entity and keyword channels to improve LLM generation. HippoRAG [14] constructs a KG by extracting triplets from the text chunks using LLMs and enhances its quality by linking similar entities via semantic embeddings. For multi-hop reasoning, it employs PPR to retrieve relevant KG entities and augments the response with entities’ associated text chunks for LLM generation.

## 6 Conclusion

In this work, we propose CUE-RAG, a graph-based RAG approach that features a multi-partite graph index integrating chunks, knowledge units, and entities. To efficiently build this index, we introduce a hybrid extraction strategy for knowledge unit that maximizes LLM processing benefits while minimizing token usage. For retrieval, we design a query-driven iterative retrieval (Q-Iter) that ensures relevant retrieval results. These designs enhance graph quality and retrieval relevance while reducing LLM token consumption. Experimental results on three QA benchmarks demonstrate that CUE-RAG significantly outperforms SOTA baselines in both QA performance and cost efficiency. Notably, its zero-token variant achieves comparable or superior performance, highlighting the robustness and effectiveness of our approach.

## References

- [1] John R Anderson. 1983. A spreading activation theory of memory. *Journal of verbal learning and verbal behavior* 22, 3 (1983), 261–295.
- [2] Akari Asai, Zeqiu Wu, Yizhong Wang, Avirup Sil, and Hannaneh Hajishirzi. 2023. Self-rag: Learning to retrieve, generate, and critique through self-reflection. In *The Twelfth International Conference on Learning Representations*.
- [3] Jinze Bai, Shuai Bai, Yunfei Chu, Zeyu Cui, Kai Dang, Xiaodong Deng, Yang Fan, Wenbin Ge, Yu Han, Fei Huang, et al. 2023. Qwen technical report. *arXiv preprint arXiv:2309.16609* (2023).
- [4] Steven Bird, Ewan Klein, and Edward Loper. 2009. *Natural Language Processing with Python: Analyzing Text with the Natural Language Toolkit*. O'Reilly Media, Inc. <https://www.nltk.org/book/>
- [5] Jianlv Chen, Shitao Xiao, Peitian Zhang, Kun Luo, Defu Lian, and Zheng Liu. 2024. BGE M3-Embedding: Multi-Lingual, Multi-Functionality, Multi-Granularity Text Embeddings Through Self-Knowledge Distillation. arXiv:2402.03216 [cs.CL]
- [6] Allan M Collins and Elizabeth F Loftus. 1975. A spreading-activation theory of semantic processing. *Psychological review* 82, 6 (1975), 407.
- [7] DeepSeek-AI, Aixin Liu, Bei Feng, Bing Xue, Bingxuan Wang, Bochao Wu, Chengda Lu, Chenggang Zhao, Chengqi Deng, Chenyu Zhang, Chong Ruan, Damai Dai, Daya Guo, Dejian Yang, Deli Chen, Dongjie Ji, Erhang Li, Fangyun Lin, Fucang Dai, Fulli Luo, Guangbo Hao, Guanting Chen, Guowei Li, H. Zhang, Han Bao, Hanwei Xu, Haocheng Wang, Haowei Zhang, Honghui Ding, Huajian Xin, Huazuo Gao, Hui Li, Hui Qu, J. L. Cai, Jian Liang, Jianzhong Guo, Jiaqi Ni, Jiashi Li, Jiawei Wang, Jin Chen, Jingchang Chen, Jingyuan Yuan, Junjie Qiu, Junlong Li, Junxiao Song, Kai Dong, Kai Hu, Kaige Gao, Kang Guan, Kexin Huang, Kuai Yu, Lean Wang, Lecong Zhang, Lei Xu, Leyi Xia, Liang Zhao, Litong Wang, Liyue Zhang, Meng Li, Miaojuan Wang, Mingchuan Zhang, Minghua Zhang, Minghui Tang, Mingming Li, Ning Tian, Panpan Huang, Peiyi Wang, Peng Zhang, Qiancheng Wang, Qihao Zhu, Qinyu Chen, Qiusi Du, R. J. Chen, R. L. Jin, Ruiqi Ge, Ruisong Zhang, Ruizhe Pan, Runji Wang, Runxin Xu, Ruoyu Zhang, Ruyi Chen, S. S. Li, Shanghao Lu, Shangyan Zhou, Shanhuang Chen, Shaoqing Wu, Shengfeng Ye, Shengfeng Ye, Shirong Ma, Shiyu Wang, Shuang Zhou, Shuiping Yu, Shunfeng Zhou, Shutong Pan, T. Wang, Tao Yun, Tian Pei, Tianyu Sun, W. L. Xiao, Wending Zeng, Wanjia Zhao, Wei An, Wen Liu, Wenfeng Liang, Wenjun Gao, Wenqin Yu, Wentao Zhang, X. Q. Li, Xiangyue Jin, Xianzu Wang, Xiao Bi, Xiaodong Liu, Xiaohan Wang, Xiaojin Shen, Xiaokang Chen, Xiaokang Zhang, Xiaosha Chen, Xiaotao Li, Xiaowen Sun, Xiaoxiang Wang, Xin Cheng, Xin Liu, Xin Xie, Xingchao Liu, Xingkai Yu, Xinnan Song, Xinxia Shan, Xinyi Zhou, Xinyu Yang, Xinyuan Li, Xuecheng Su, Xuheng Lin, Y. K. Li, Y. Q. Wang, Y. X. Wei, Y. X. Zhu, Yang Zhang, Yanhong Xu, Yanhong Xu, Yanping Huang, Yao Li, Yao Zhao, Yaofeng Sun, Yaohui Li, Yaohui Wang, Yi Yu, Yi Zheng, Yichao Zhang, Yifan Shi, Yiliang Xiong, Ying He, Ying Tang, Yishi Piao, Yisong Wang, Yixuan Tan, Yiyang Ma, Yiyuan Liu, Yongqiang Guo, Yu Wu, Yuan Ou, Yuchen Zhu, Yudian Wang, Yue Gong, Yuheng Zou, Yujia He, Yukun Zha, Yunfan Xiong, Yuxian Ma, Yuting Yan, Yuxiang Luo, Yuxiang You, Yuxuan Liu, Yuyang Zhou, Z. F. Wu, Z. Z. Ren, Zehui Ren, Zhaogli Sha, Zhe Fu, Zhean Xu, Zhen Huang, Zhen Zhang, Zhenda Xie, Zhengyan Zhang, Zhewen Hao, Zhibin Gou, Zhicheng Ma, Zhigang Yan, Zhihong Shao, Zhipeng Xu, Zhiyu Wu, Zhongyu Zhang, Zhuoshu Li, Zihui Gu, Zijia Zhu, Zijun Liu, Zilin Li, Ziwei Xie, Ziyang Song, Ziyi Gao, and Zizheng Pan. 2025. DeepSeek-V3 Technical Report. arXiv:2412.19437 [cs.CL] <https://arxiv.org/abs/2412.19437>
- [8] Darren Edge, Ha Trinh, Newman Cheng, Joshua Bradley, Alex Chao, Apurva Mody, Steven Truitt, Dasha Metropolitan, Robert Osazuwa Ness, and Jonathan Larson. 2024. From local to global: A graph rag approach to query-focused summarization. *arXiv preprint arXiv:2404.16130* (2024).
- [9] Wenqi Fan, Yujuan Ding, Liangbo Ning, Shijie Wang, Hengyun Li, Dawei Yin, Tat-Seng Chua, and Qing Li. 2024. A survey on rag meeting llms: Towards retrieval-augmented large language models. In *Proceedings of the 30th ACM SIGKDD Conference on Knowledge Discovery and Data Mining*. 6491–6501.
- [10] Yunfan Gao, Yun Xiong, Xinyu Gao, Kangxiang Jia, Jinliu Pan, Yuxi Bi, Yixin Dai, Jiawei Sun, Haofen Wang, and Haofen Wang. 2023. Retrieval-augmented generation for large language models: A survey. *arXiv preprint arXiv:2312.10997* 2, 1 (2023).
- [11] Aashish Ghimire, James Pather, and John Edwards. 2024. Generative AI in education: A study of Educators' awareness, sentiments, and influencing factors. In *2024 IEEE Frontiers in Education Conference (FIE)*. IEEE, 1–9.
- [12] Aaron Grattafiori, Abhimanyu Dubey, Abhinav Jauhri, Abhinav Pandey, Abhishek Kadian, Ahmad Al-Dahle, Aiesha Letman, Akhil Mathur, Alan Schelten, Alex Vaughan, et al. 2024. The llama 3 herd of models. *arXiv preprint arXiv:2407.21783* (2024).
- [13] Zirui Guo, Lianghao Xia, Yanhua Yu, Tu Ao, and Chao Huang. 2024. Lightrag: Simple and fast retrieval-augmented generation. (2024).
- [14] Bernal Jiménez Gutiérrez, Yiheng Shu, Yu Gu, Michihiro Yasunaga, and Yu Su. 2024. Hipporag: Neurobiologically inspired long-term memory for large language models. In *The Thirty-eighth Annual Conference on Neural Information Processing Systems*.
- [15] Xiaoxin He, Yijun Tian, Yifei Sun, Nitesh Chawla, Thomas Laurent, Yann LeCun, Xavier Bresson, and Bryan Hooi. 2024. G-retriever: Retrieval-augmented generation for textual graph understanding and question answering. *Advances in Neural Information Processing Systems* 37 (2024), 132876–132907.
- [16] Xanh Ho, Anh-Khoa Duong Nguyen, Saku Sugawara, and Akiko Aizawa. 2020. Constructing a multi-hop qa dataset for comprehensive evaluation of reasoning steps. *arXiv preprint arXiv:2011.01060* (2020).
- [17] Matthew Honnibal, Ines Montani, Sofie Van Landeghem, and Adriane Boyd. 2020. spaCy: Industrial-strength Natural Language Processing in Python. (2020). doi:10.5281/zenodo.1212303
- [18] Yucheng Hu and Yuxing Lu. 2024. Rag and rau: A survey on retrieval-augmented language model in natural language processing. *arXiv preprint arXiv:2404.19543* (2024).
- [19] Yizheng Huang and Jimmy Huang. 2024. A survey on retrieval-augmented text generation for large language models. *arXiv preprint arXiv:2404.10981* (2024).
- [20] Yiqian Huang, Shiqi Zhang, and Xiaokui Xiao. 2025. KET-RAG: A Cost-Efficient Multi-Granular Indexing Framework for Graph-RAG. *arXiv preprint arXiv:2502.09304* (2025).
- [21] Lei Liu, Xiaoyan Yang, Junchi Lei, Xiaoyang Liu, Yue Shen, Zhiqiang Zhang, Peng Wei, Jinjie Gu, Zhixuan Chu, Zhan Qin, et al. 2024. A survey on medical large language models: Technology, application, trustworthiness, and future directions. *arXiv preprint arXiv:2406.03712* (2024).
- [22] Nelson F Liu, Kevin Lin, John Hewitt, Ashwin Paranjape, Michele Bevilacqua, Fabio Petroni, and Percy Liang. 2023. Lost in the middle: How language models use long contexts. *arXiv preprint arXiv:2307.03172* (2023).
- [23] Alex Mallen, Akari Asai, Victor Zhong, Rajarshi Das, Daniel Khoshabi, and Hannaneh Hajishirzi. 2022. When not to trust language models: Investigating effectiveness of parametric and non-parametric memories. *arXiv preprint arXiv:2212.10511* (2022).
- [24] Leland McInnes, John Healy, and James Melville. 2018. Umap: Uniform manifold approximation and projection for dimension reduction. *arXiv preprint arXiv:1802.03426* (2018).
- [25] Nebula. 2010. nebula. <https://www.nebula-graph.io/>. Accessed: [Insert Access Date].
- [26] Neo4j. 2006. neo4j. <https://neo4j.com/>. Accessed: [Insert Access Date].
- [27] Yuqi Nie, Yaxuan Kong, Xiaowen Dong, John M Mulvey, H Vincent Poor, Qing-song Wen, and Stefan Zohren. 2024. A survey of large language models for financial applications: Progress, prospects and challenges. *arXiv preprint arXiv:2406.11903* (2024).
- [28] OpenAI. [n. d.]. tiktoken. <https://github.com/openai/tiktoken>
- [29] Kishore Papineni, Salim Roukos, Todd Ward, and Wei-Jing Zhu. 2002. Bleu: a method for automatic evaluation of machine translation. In *Proceedings of the 40th annual meeting of the Association for Computational Linguistics*. 311–318.
- [30] Boci Peng, Yun Zhu, Yongchao Liu, Xiaohe Bo, Haizhou Shi, Chuntao Hong, Yan Zhang, and Siliang Tang. 2024. Graph retrieval-augmented generation: A survey. *arXiv preprint arXiv:2408.08921* (2024).
- [31] Ofir Press, Muru Zhang, Sewon Min, Ludwig Schmidt, Noah A Smith, and Mike Lewis. 2022. Measuring and narrowing the compositionality gap in language models. *arXiv preprint arXiv:2210.03350* (2022).
- [32] Ori Ram, Yoav Levine, Itay Dalmedigos, Dorn Muhlgay, Amnon Shashua, Kevin Leyton-Brown, and Yoav Shoham. 2023. In-context retrieval-augmented language models. *Transactions of the Association for Computational Linguistics* 11 (2023), 1316–1331.
- [33] Sartaj Sahni. 1975. Approximate algorithms for the 0/1 knapsack problem. *Journal of the ACM (JACM)* 22, 1 (1975), 115–124.
- [34] Parth Sarthi, Salman Abdullah, Aditi Tuli, Shubh Khanna, Anna Goldie, and Christopher D Manning. 2024. Raptor: Recursive abstract processing for tree-organized retrieval. In *The Twelfth International Conference on Learning Representations*.
- [35] Vincent A Traag, Ludo Waltman, and Nees Jan Van Eck. 2019. From Louvain to Leiden: guaranteeing well-connected communities. *Scientific reports* 9, 1 (2019), 1–12.
- [36] Harsh Trivedi, Niranjan Balasubramanian, Tushar Khot, and Ashish Sabharwal. 2022. Interleaving retrieval with chain-of-thought reasoning for knowledge-intensive multi-step questions. *arXiv preprint arXiv:2212.10509* (2022).
- [37] Harsh Trivedi, Niranjan Balasubramanian, Tushar Khot, and Ashish Sabharwal. 2022. MuSiQue: Multihop Questions via Single-hop Question Composition. *Transactions of the Association for Computational Linguistics* 10 (2022), 539–554.
- [38] Shu Wang, Yixiang Fang, Yingli Zhou, Xilin Liu, and Yuchi Ma. 2025. ArchRAG: Attributed Community-based Hierarchical Retrieval-Augmented Generation. arXiv:2502.09891 [cs.IR] <https://arxiv.org/abs/2502.09891>
- [39] Shen Wang, Tianlong Xu, Hang Li, Chaoli Zhang, Joleen Liang, Jiliang Tang, Philip S Yu, and Qingsong Wen. 2024. Large language models for education: A survey and outlook. *arXiv preprint arXiv:2403.18105* (2024).
- [40] Shangyu Wu, Ying Xiong, Yufei Cui, Haolun Wu, Can Chen, Ye Yuan, Lianming Huang, Xue Liu, Tei-Wei Kuo, Nan Guan, et al. 2024. Retrieval-augmented generation for natural language processing: A survey. *arXiv preprint arXiv:2407.13193* (2024).

- [41] Zhishang Xiang, Chuanjie Wu, Qinggang Zhang, Shengyuan Chen, Zijin Hong, Xiao Huang, and Jinsong Su. 2025. When to use Graphs in RAG: A Comprehensive Analysis for Graph Retrieval-Augmented Generation. *arXiv preprint arXiv:2506.05690* (2025).
- [42] An Yang, Anfeng Li, Baosong Yang, Beichen Zhang, Binyuan Hui, Bo Zheng, Bowen Yu, Chang Gao, Chengen Huang, Chenxu Lv, et al. 2025. Qwen3 technical report. *arXiv preprint arXiv:2505.09388* (2025).
- [43] Zhilin Yang, Peng Qi, Saizheng Zhang, Yoshua Bengio, William W Cohen, Ruslan Salakhutdinov, and Christopher D Manning. 2018. HotpotQA: A dataset for diverse, explainable multi-hop question answering. *arXiv preprint arXiv:1809.09600* (2018).
- [44] Hao Yu, Aoran Gan, Kai Zhang, Shiwei Tong, Qi Liu, and Zhaofeng Liu. 2024. Evaluation of retrieval-augmented generation: A survey. In *CCF Conference on Big Data*. Springer, 102–120.
- [45] Nan Zhang, Prafulla Kumar Choubey, Alexander Fabbri, Gabriel Bernadett-Shapiro, Rui Zhang, Prasenjit Mitra, Caiming Xiong, and Chien-Sheng Wu. 2024. SiReRAG: Indexing Similar and Related Information for Multihop Reasoning. *arXiv preprint arXiv:2412.06206* (2024).
- [46] Qinggang Zhang, Shengyuan Chen, Yuanchen Bei, Zheng Yuan, Huachi Zhou, Zijin Hong, Junnan Dong, Hao Chen, Yi Chang, and Xiao Huang. 2025. A Survey of Graph Retrieval-Augmented Generation for Customized Large Language Models. *arXiv preprint arXiv:2501.13958* (2025).
- [47] Penghao Zhao, Hailin Zhang, Qinhan Yu, Zhengren Wang, Yunteng Geng, Fangcheng Fu, Ling Yang, Wentao Zhang, Jie Jiang, and Bin Cui. 2024. Retrieval-augmented generation for ai-generated content: A survey. *arXiv preprint arXiv:2402.19473* (2024).
- [48] Yingli Zhou, Yaodong Su, Youran Sun, Shu Wang, Taotao Wang, Runyuan He, Yongwei Zhang, Sicong Liang, Xilin Liu, Yuchi Ma, et al. 2025. In-depth Analysis of Graph-based RAG in a Unified Framework. *arXiv preprint arXiv:2503.04338* (2025).

## A Supplementary Details

Table 5 presents the key statistics for the three benchmark datasets used in our study: MuSiQue, HotpotQA, and 2Wiki, including corpora size, number of questions, and total token count. Table 6 reports the node counts for the CUE-RAG-1.0 graph index, detailing the quantities of text nodes, *knowledge unit* nodes, and entity nodes for each dataset. Algorithm 4 provides the complete pseudocode for the Entity-Anchoring procedure. Figure 7 and 8 illustrate the LLM instruction prompts used for extracting *knowledge units* and answer generations, respectively.

**Table 5: Details of three benchmark datasets.**

Dataset	MuSiQue	HotpotQA	2Wiki
Questions	1,000	1,000	1,000
Passages	11,656	9,221	6,119
Tokens	1,281,422	1,239,838	640,205

**Table 6: Statistics of CUE-RAG-1.0’s graph index in LLaMA3.0-8B and Qwen2.5-32B.**

Model	Nodes	MuSiQue	HotpotQA	2Wiki
LLaMA 3.0-8B	Texts	11,656	9,221	6,119
	Knowledge	108,513	100,789	52,149
	Entities	222,940	209,869	123,116
Qwen 2.5-32B	Texts	11,656	9,221	6,119
	Knowledge	114,256	108,957	57,442
	Entities	238,954	229,762	136,966

---

### Algorithm 4: Entity-Anchoring ( $q, \mathcal{G}, K$ )

---

- 1 **Input:** query  $q$ , number of most relevant results  $K$ ,  
hierarchical graph index  $\mathcal{G} = (\mathcal{V}_{\mathcal{T}} \cup \mathcal{V}_{\mathcal{K}} \cup \mathcal{V}_{\mathcal{E}}, \mathcal{E}_c \cup \mathcal{E}_e)$
- 2 **Output:** initial seed nodes  $\mathcal{V}_q^{(0)}$
- 3 # Spreading Activation
- 4  $\mathcal{V}_q \leftarrow \text{NER}(q); \mathcal{V}_q^{(0)} \leftarrow \emptyset;$
- 5 **foreach**  $v \in \mathcal{V}_q$  **do**
- 6      $\mathcal{N}_v \leftarrow \arg \max_{v' \in \mathcal{V}_e \wedge |\mathcal{N}_v|=K} \cos(\phi(v'), \phi(v));$
- 7      $\mathcal{V}_q^{(0)} \leftarrow \mathcal{V}_q^{(0)} \cup \mathcal{N}_v;$
- 8 # Knowledge Anchoring
- 9  $\mathcal{K}_q \leftarrow \arg \max_{k \in \mathcal{V}_{\mathcal{K}} \wedge |\mathcal{K}_q|=K} \cos(\phi(k), \phi(q));$
- 10  $\mathcal{V}_q^{(0)} \leftarrow \mathcal{V}_q^{(0)} \cup \bigcup_{k \in \mathcal{K}_q} \{v \mid (v, k) \in \mathcal{E}_e\};$
- 11 **return**  $\mathcal{V}_q^{(0)}$

---

Prompt for generating knowledge units

**Prompt:**

Decompose the content into clear knowledge units, ensuring they are interpretable independently of their original context:

- (1) Sentence Simplification: Break compound sentences into simpler, individual sentences. Whenever possible, retain the original phrasing from the input text.
- (2) Entity and Description Separation: For named entities that are accompanied by descriptive information, separate the descriptive details into a distinct knowledge unit. Ensure each knowledge unit represents a single, clear fact.
- (3) Pronoun Resolution: Replace all pronouns (e.g., "it", "they", "this") with explicit references, using full taxonomic names or clear identifiers. Always use "[entity]'s [property]" construction.
- (4) Output Format: Present the resulting knowledge units as a list of strings, formatted in JSON.

**EXAMPLE-1:**

Input:

Jesúfas Aranguren. His 13-year professional career was solely associated with Athletic Bilbao, with which he played in nearly 400 official games, winning two Copa del Rey trophies.

Output:

```
{
  "knowledge units": [
    "Jesús Aranguren had a 13-year professional career.",
    "Jesús Aranguren's professional career was solely associated with Athletic Bilbao.",
    "Athletic Bilbao is a football club.",
    "Jesús Aranguren played for Athletic Bilbao in nearly 400 official games.",
    "Jesús Aranguren won two Copa del Rey trophies with Athletic Bilbao.",
  ]
}
```

**EXAMPLE-2:**

Input:

Ophrys apifera. Ophrys apifera grows to a height of 15 – 50 centimetres (6 – 20 in). This hardy orchid develops small rosettes of leaves in autumn. They continue to grow slowly during winter. Basal leaves are ovate or oblong - lanceolate, upper leaves and bracts are ovate - lanceolate and sheathing. The plant blooms from mid-April to July producing a spike composed from one to twelve flowers. The flowers have large sepals, with a central green rib and their colour varies from white to pink, while petals are short, pubescent, yellow to greenish. The labellum is trilobed, with two pronounced humps on the hairy lateral lobes, the median lobe is hairy and similar to the abdomen of a bee. It is quite variable in the pattern of coloration, but usually brownish - red with yellow markings. The gynostegium is at right angles, with an elongated apex.

Output:

```
{
  "knowledge units": [
    "Ophrys apifera grows to a height of 15-50 centimetres (6-20 in)",
    "Ophrys apifera is a hardy orchid",
    "Ophrys apifera develops small rosettes of leaves in autumn",
    "The leaves of Ophrys apifera continue to grow slowly during winter",
    "The basal leaves of Ophrys apifera are ovate or oblong-lanceolate",
    "The upper leaves and bracts of Ophrys apifera are ovate-lanceolate and sheathing",
    "Ophrys apifera blooms from mid-April to July",
    "Ophrys apifera produces a spike composed of one to twelve flowers",
    "The flowers of Ophrys apifera have large sepals with a central green rib",
    "The flowers of Ophrys apifera vary in colour from white to pink",
    "The petals of Ophrys apifera are short, pubescent, and yellow to greenish",
    "The labellum of Ophrys apifera is trilobed with two pronounced humps on the hairy lateral lobes",
    "The median lobe of Ophrys apifera's labellum is hairy and resembles a bee's abdomen",
    "The coloration pattern of Ophrys apifera is variable but usually brownish-red with yellow markings",
    "The gynostegium of Ophrys apifera is at right angles with an elongated apex" ,
  ]
}
```

JUST OUTPUT THE RESULTS IN JSON FORMAT!

Input: {passage}

Output:

Figure 7: The prompt for generating knowledge units.

Prompt for answer generation

**Prompt:**

Your goal is to give the best full answer to question the user input according to the given context below.

Given Context: {context}

Give the best full answer to question :{question}

Answer this question in as fewer number of words as possible.

**Figure 8: The prompt for generating answer.**